Non linear seismic analysis of charge/discharge machine

M.Dostal
National Nuclear Corporation Ltd, Warrington, UK
V.M.Trbojevic
Technica Dynamics Ltd, London, UK
M.Nobile
Ente Nazionale per l'Energia Elettrica, Rome, Italy

1. INTRODUCTION

The Magnox Nuclear Power Station at Latina has undergone a design re-appraisal under revised seismic loadings. As part of this exercise the charge/discharge machine (CDM) has been analysed in three stages. Initially, a conservative, linear response spectrum analysis was carried out to assess the global response. This was followed by more detailed static stress analysis of structural members and components. The linear analysis necessitated a number of simplifying assumptions which on one hand are over-conservative and on the other lead to unrealistic dynamic behaviour. This paper describes the third phase of the analysis where the non-linear features of the CDM were taken into account.

2. FINITE ELEMENT MODEL OF CDM

The CDM consists of a tall shielded pressure vessel supported on a bogie which travels on 28m long gantry beams, Figure 1. One end of the beam is supported on a 'fixed leg' the other on a so-called 'hinged leg', which allows rotation and also vertical separation. The dead weight of the CDM is transmitted to the bogies via a pair of 'rocker pads', which can also transmit horizontal forces. However, these open type rocker pads permit a vertical separation and a sliding movement between the wheels and the rail is possible.

The finite element model of the CDM consists of 178 beam elements and 28 trusses, having altogether 728 degrees-of-freedom. The CDM model with cross-travel bogie in the central position is shown in Figure 2. The finite element representation of the cross-travel bogie is shown in Figure 3. The bogie supports the vertical charge machine with rigid beams. The bogie is modelled by beam elements, except for the elements representing rocker pads, and the elements representing connecting wheels, which are modelled by trusses. There are eight rocker pads as numbered in Figure 3, each of which is represented as a contact-gap element withstanding axial compression only and allowing separation; vertical beams connect wheels at the top of a gantry beam to its neutral axis, accounting for the beam height and having a contact/friction boundary condition. The inside wheels have brakes which are represented by a friction element and are marked by letter F in Figure 3.

The hinged leg of the gantry model is shown in Figure 4. The rocker pads are numbered from 9 to 12. The wheels have brakes applied to inside pairs (marked by a letter F) modelled as contact/friction elements. The rotation around Z axis is released at 'hinge nodes'. The rotation about Y axis is released at the bogies at nodes marked by letter R.

The charge machine shielding and pressure vessel are essentially concentric rings which have been modelled by two lines of beam elements linked by a shorter element to represent bolts. The lower end of this vessel is connected to the stand pipes via a head box which allows vertical translation (X direction) and all rotations.

The model of the CDM with the cross-travel bogie above the hinged leg is derived from the original model, Figure 2, by shifting the cross-travel to the hinged end and re-arranging the discretization of the gantry beams.

3. TREATMENT OF CONTACTS WITH FRICTION

There are various methods of treatment for the contact/friction problems, examples of which, extracted from the vast amount of literature, are those by Hughes et al [1], Oden and Kikuchi [2], Klarbring [3], Torstenfelt [4], and Fredriksson [5]. The non-penetration condition during contact is a unilateral boundary condition on relative displacements and constitutes a complicated non-linear problem. Friction is simulated by a 'constitutive relation' for the contact stress and relative displacement behaviour on the contact surface. The basic assumption for the constitutive relations for the contact surface states that there exists a a slip criterion of the form

$$f(\tau) = \|\tau_s\| + \mu \tau_n, \quad f(\tau) < 0 \qquad (1)$$

where τ is the traction vector with components in the tangential and normal directions, τ_s and τ_n respectively, and μ is the coefficient of friction. An associated flow rule relates the tangential velocity U_s with the tangential traction τ_s as follows:

$$U_s = \lambda \frac{\partial f(\tau)}{\partial \tau_s} \quad (\lambda > 0) \qquad (2)$$

The kinematic condition for contact to take place between bodies A and B along the contact surface C requires

$$U_n^A - U_n^B - \delta = 0 \qquad (3)$$

where U_n is the normal component of the displacement U, and δ is an initial relative displacement (gap). When this condition is satisfied within some specified tolerance, two cases may occur:

adhesion $\quad U_s^A - U_s^B = 0 \qquad (4)$
$\quad f(\tau) < 0$ on C,

and sliding $\quad U_s^A - U_s^B = \lambda \tau_s \qquad (5)$
$\quad f(\tau) = 0$ on C

Spatial discretization of bodies is achieved by a standard finite element technique. Contact force is included in the global matrix equations via the Lagrangian multiplier technique which gives rise to a so-called 'contact element stiffness matrix' [1]. This results in a system of non-linear ordinary differential equations which are discretized in time using the Newmark algorithm, and solved in each time step by the Newton-Raphson technique.

4. SEISMIC EXCITATION AND BASIC PARAMETERS

The response spectra are presented in Figure 5, for the three coordinate directions. The time domain seismic response analyses were performed with the time step of 0.05s. Full Raleigh damping was applied as 5% of critical damping at 1.2Hz. The friction coefficient was 0.3.

As the CDM consists of six sub-structures connected via open hinges and a number of rocker pads, the stability of the complete assembly is essentially dependent on gravitational forces. The stability criteria for the complete assembly and substructures have been defined in terms of maximum horizontal displacements.

5. SEISMIC RESPONSE ANALYSIS

The non-linear time-marching analysis was performed for the two cases selected for this study:

A. CDM located centrally. Acceleration time history corresponding to 0.07g peak ground acceleration

B. CDM located over hinged leg. Acceleration time history corresponding to 0.07g peak ground acceleration.

Similar analysis was also performed with the time histories scaled up to 0.1g peak ground acceleration.

6. RESULTS

For each of the analyses conditions specified previously a large number of displacement-time histories were monitored. A summary of the displacement amplitudes minima and maxima is presented in Table 1. The transverse oscillations (Z direction) are governed by the first mode, f = 1.1Hz, and the longitudinal oscillations by the second mode, f = 1.7Hz. Sliding of the cross-travel bogie, with a realistic upper bound estimate of 0.3 for the coefficient of friction, was 2mm when the CDM was located centrally.

The maximum values of the separation of the rocker pads is given in Table 2. The maximum separation of the cross-travel bogie is about 12mm, and on the fixed leg about 14mm. Separation at the hinged leg is negligible.

To show the rocking of the cross-travel bogie time histories of the rocker pad differential displacements are superimposed for the rocker pads 1 and 6, respectively, as shown in Figure 6, for the analysis condition A. The dominant rocking mode about Y axis at f = 1.2Hz can be identified. Rocking at the fixed leg is presented in Figure 7, in which the time histories of the inner and outer (with respect to the rail) rocker pad differential displacements are superimposed. It is important to notice that the rocking of inner and outer rocker pads is not in phase. This means that the fixed leg would be stable even if the maximum separation exceeded the conservatively-defined stability limit because the separation would always take place on one side only, while the pad on the other side would be engaged.

7. CONCLUSIONS

The main conclusions of the seismic analysis of the Latina CDM are:-

i. The charge machine has been demonstrated to be capable of withstanding the effects of a 0.1g earthquake. Stresses and displacements were all within allowable limits and the stability criteria were fully satisfied for all positions of the cross-travel bogie on the gantry.

ii. Movements due to loss of friction between the cross-travel bogie wheels and the rail was found to be small; i.e. less than 2mm for all cases considered. The modes of rocking of the fixed and hinged legs preclude any possibility of excessive movement between the long travel bogie wheels and the rail.

iii. The non-linear analysis incorporating contact and friction has given more realistic results than any of the linear verification analyses. The method of analysis indicates that even the larger structures can be efficiently solved on a mini computer for a long forcing input (16s).

REFERENCES

[1] Hughes, T.J.R. et al. 1976. Finite Element Models for Large Displacement Contact-Impact Analysis. SESM Report No, 76-4, University of California, Berkeley.

[2] Oden, J.T., and Kikuchi, W. 1982. Finite Element Methods for Constrained Problems in Elasticity. Int. J. Num. Meth. Eng., 18, 701-725.

[3] Klarbring, A. 1982. Variational Principles of Contact Mechanics. Linkoping Institute of Technology, Report LiTH-IKP-R-263.

[4] Torstenfelt, B. 1983. Contact Problems with Friction in General Purpose Finite Element Computer Programs. Comp. & Struct., Vol. 16, No. 1-4, pp 487-493.

[5] Fredriksson, B. et al. 1984. Numerical Solutions to Contact, Friction and Crack Problems with Applications. Engineering Computations, Vol. 1, No. 2, pp. 133-143.

Table 1 : Displacement Amplitudes [mm]

Position	Direction	Analysis A	Analysis B
Gantry	Y	±30	±31
	Y	±32	±32
Hinged Leg	Y	±30	±30
Fixed Leg	Y	±30	±30
	Z	±35	±56
Head-Box	Y	±33	±28
	Z	±29	±21

Table 2 : Maximum Values of the Rocker Pads Differential Displacements (Gaps)[mm]

Pad No.	Position	Analysis A	Analysis B
1	Cross-travel	10.0	5.8
2	Bogie +Z side	5.2	7.5
3		3.6	6.9
4		10.8	6.6
5	Cross-travel	6.0	8.0
6	Bogie -Z side	11.5	5.8
7		11.0	5.8
8		4.6	7.9
9	Hinged Leg	0.0	0.0
10		0.2	0.0
11		1.1	0.5
12		0.9	0.6
13	Fixed Leg	13.8	24.1
14		13.9	24.8
15		13.7	22.9
16		12.7	22.9

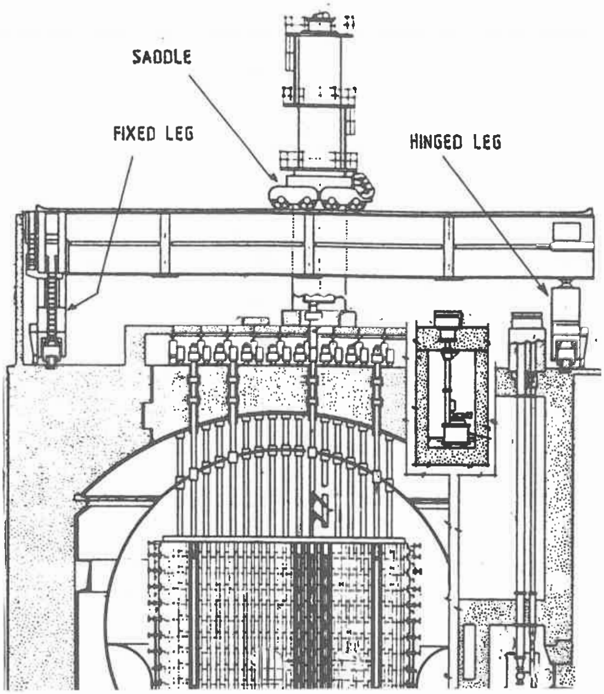

Figure 1: Latina Charge/Discharge Machine

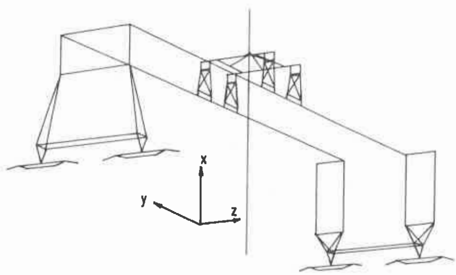

Figure 2: Computational Model of the Latina CDM

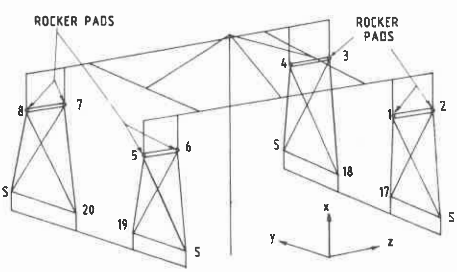

Figure 3: Model of the Cross-Travel Bogie

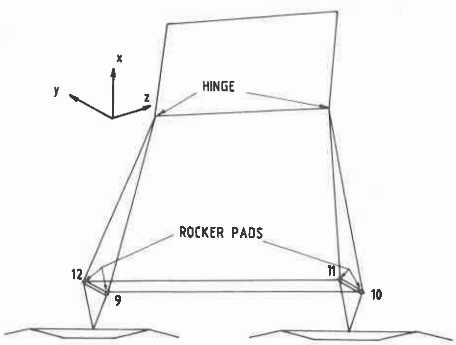

Figure 4: Model of the Hinged Leg

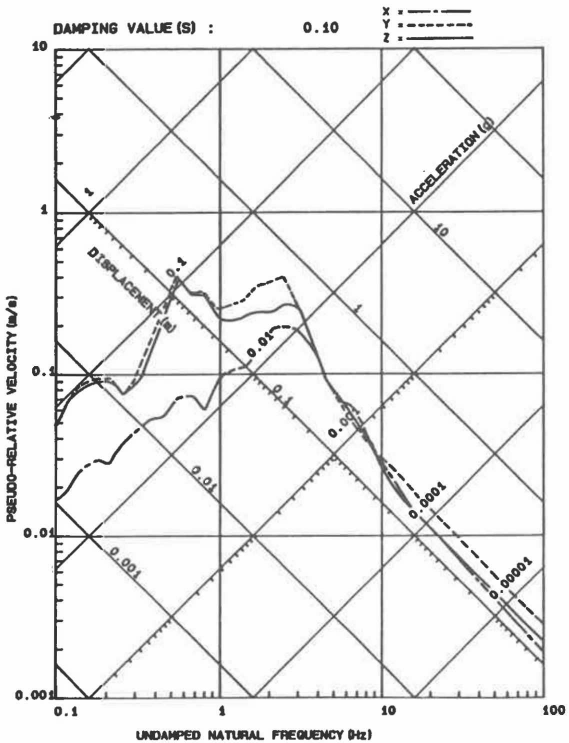

Figure 5: Input Motion Response Spectra

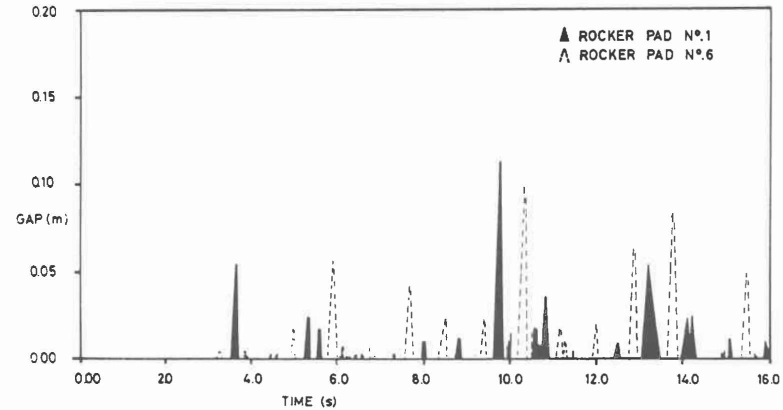

Figure 6: Differential Displacement Time Histories at Rocker Pads 1 and 6

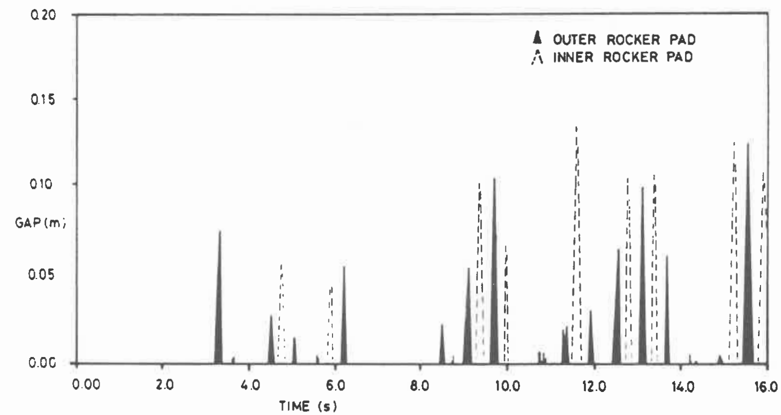

Figure 7: Differential Displacement Time Histories at the Fixed Leg